Abstract

Printable stretchable devices, which can be used in a wide range of environments, are required for a range of flexible or stretchable electronics applications. Here we present an ink containing liquid exfoliated graphene and natural rubber, which can be printed onto a variety of elastomeric substrates and recover conductance after multiple strains of up to 15%. In addition, the printed composite acts as a strain sensor with a gauge factor of around 7. The robust character of these composites allows for operation at temperatures up to 150ºC. The combination of the effectiveness of the device, along with comparable performance at elevated temperatures while being relatively cheap makes this ideal for integration with automotive components. For applications that require superior conductivity, silver nanowires can be added. The enhanced conductivity composite cannot withstand higher temperatures due to the breakdown of the nanowires. However, at room temperature the material shows similar recovery of conductivity after cycling leading to a highly conductive, room temperature, printable, stretchable composite.

1. Introduction

Elastomeric materials are ubiquitous in modern domestic and industrial equipment. Prime examples of these being automobile components and medical devices, such as tyres and tubing. Recent research has turned towards integration in wearable electronics[1]. A material that resists conductance changes after straining is of interest for passive devices, for instance RFIDs, while the variation of conductance with strain allows for integration as a strain gauge. Importantly, the material should function with the practical strain range of the substrate to which it is adhered.

Elastomeric nanocomposites are a class of materials that fit the requirements for such devices. These materials have been extensively studied as strain sensors[1–3]. Strain sensors operate by exhibiting a change in electrical resistance as the material is strained. For elastomeric composites with high aspect ratio conductive nanoparticulate fillers the mechanism is a combination of severing of conductive connections and tunnelling between the filler particles[1]. The gauge factor (G) is defined by equations 1 & 2.

$$G = \frac{\Delta R}{R_0 \varepsilon} \qquad \text{Equation 1}$$

$$G = 1 + 2\nu + \frac{\Delta \rho}{\rho_0 \varepsilon} \qquad \text{Equation 2}$$

Where R and ρ represent resistances and resistivities respectively, ε is the strain and υ is the Poisson's ratio of the material. Traditional metal foil strain gauges have an operating range of below 2% and a gauge factor of 2-3. Elastomeric strain gauges have both higher operating strains and gauge factors and have recently been the focus of intensive research[1–3].

The most common and well-studied fillers for elastomeric composites in recent years are carbon nanotubes[4–6] (CNTs) and graphene[7–9]. Both materials have high conductivities and aspect ratios. This allows mechanical reinforcement at low mass fractions[5,8] and the addition of conductivity to the bulk at mass fractions exceeding a percolation threshold[9,10]. These materials have been utilised as strain sensors as both surface coatings and as composite materials[1,2]. Another material of interest are silver nanowires (AgNWs). AgNWs are high aspect ratio wires of silver synthesised by the reduction of silver salts in the presence of capping material to promote unidirectional growth[11]. The first major application of this material was as transparent conductors[12,13] and has since progressed to have significant applications in strain sensing and in conducting composites[14,15].

Nanomaterials networks alone are not suitable for high strain applications due to both poor substrate adhesion and low strain at break[16]. This leads to the introduction of the elastomer matrix to address these issues. For elastomeric products that require conductive tracks and sensors a conductive ink is necessary to allow to bespoke device manufacture. This requires the materials to be processed and stable in a liquid phase to allow for printing. Graphene can be stabilised in liquids by a variety of methods[17–19]. In this work, an amphiphilic surfactant is used to stabilise the graphene particles in dispersion in water[19]. This allows for a reasonably low boiling point, printable ink to be produced; the only drawback being the presence of surfactant which has to be minimised for practical application. AgNWs have no issues with water dispersion as the capping material also acts as a surfactant[11].

Once the material is dispersed in a liquid, the printing onto the substrate is the final step. For graphene enabled inks the main methods of printing that are scalable are ink-jet printing, aerosol-jet printing and screen-printing[20,21]. The choice of printing technique mainly depends on the thickness of material required. Ink-jet and aerosol-jet printing typically are for printing thin films (<1μm) but for thicker films screen-printing is a preferable method. The viscosities required for screen-printing are also much higher in the range of 0.5-100 Pa.s. To achieve sheet resistances of less than 100Ω/□ with conductivities of order of 1000S/m[8] (typical of graphene polymer composites) thickness of at least 10μm is required and thus so is screen-printing.

In this paper, we produce printed tracks of natural rubber composites with both graphene and AgNWs as the conductive filler. The materials' static properties are optimised before printing conductive tracks on an array of elastomeric substrates and assessed as a strain-able conductor and strain gauge.

2. Materials & Methods

Graphite (CAS# 7782-42-5, D10 1.8μm, D50 6.3μm, D90 12.2μm) was obtained from Kibaran Resources Ltd. Silver nanowires (CAS# 7440-22-4,20 nm, 12 micron) were purchased from Sigma Aldrich. Natural Rubber Latex (60 wt.% solids) was purchased from Liquid Latex Direct. All other chemicals used were purchased from Sigma Aldrich (reagent grade). A commercially available rubber substrate (rubber band width 15mm, Office Depot) was used to demonstrate versatility of the process.

Graphene was produced by high shear exfoliation in a Mini DeBEE homogenizer from BEE International at 35kpsi for 10 passes using 60g/L graphite to 4g/L Triton X-100 (CAS# 9002-93-1). Full details of the dispersion procedure are published in previous work[22]. The material was centrifuged at 5000g for 6 minutes to remove large aggregates and then centrifuged at 5000g for 1 hour to remove the few layer graphene as well as leave unbound surfactant in the supernatant. The sediment formed a clay like paste which can subsequently be used as the base for the screen printing formulation. Natural rubber latex was added to the paste and homogenised by stirring and grinding. In the case of hybrid inks, AgNWs removed from solvent by centrifugation, is added to the paste in a similar manner. To elevate the boiling point of the paste and adjust viscosity (to the point that the clay became screen-printable (i.e. having a viscosity of ~ 1000-10,000cp) the paste was mixed with an equal mass of ethylene glycol (CAS# 107-21-1). The material was then screen-printed using a screen of mesh size 90T. Thickness of films was calculated using an encoded mechanical stage microscope.

All dynamic electrical measurements were carried out using a Keithley 2614B sourcemeter providing a constant potential of 10V. Static electrical measurements were performed

similarly but with voltage sweeps from -10 to 10V. To remove contact resistance from 2 probe measurements the transmission line measurement was used. The mechanical cycling were performed using a Stable Micro Systems TA-TXplus texture analyser for this study all strain cycling was done at a rate of 40%/s and individual strain analysis was done at 4%/s. Mechanical Testing under a variety of temperatures was performed using a Stable Micro Systems Thermal Cabinet.

3. Results & Discussion

The design of inks for printable stretchable electronics require both a conductive and stretchable component due to the fact that traditional elastomers are generally not conductive and traditional conductive materials generally cannot sustain high strains. The combination of natural rubber, the archetypical elastomer, and graphene, a material with excellent conductive and mechanical properties can results in a material with the desired properties of both. Formulating an ink of these materials requires liquid suspensions of these materials that can be mixed. Natural rubber is available as a liquid latex dispersion with high mass fraction. Commercial formulations include crosslinking agents allowing for facile elastomeric composite fabrication. Graphene dispersions, which are stabilised by surfactant in water allow for a mixture of these two materials for printable elastomeric conductive tracks.

In this work, a nano-particulate graphite paste (~30 wt.%), made by centrifugation of a dispersion containing few-layer and multi-layer graphene, is blended with a rubber latex to make material of given mass fractions. The graphene was characterised by UV-Vis spectrophotometry, Raman spectroscopy and dynamic light scattering shown in figure S1. From the UV-Vis data the material is shown to have an average layer number of 11.5 from

metrics derived by Backes et al[23]. Raman spectroscopy shows graphitic character with a low D/G ratio typical of liquid exfoliated graphene with a low basal plane defect density[24]. The dynamic light scattering measurements clarify the material is on the length scale of a few hundred nm to 2μm. AFM (shown in figure S2) confirms this. To adjust the viscosity for screen-printing, the composite paste is mixed with an equivalent mass of ethylene glycol. The ink is then printed onto the substrate using a manual screen-printing table. In figure 1a a track of printed material is shown. The track is approximately 1.5mm across. The printing resolution and thickness is defined by the mesh size, thickness and ink volume fraction as well as the roughness of the underlying substrate. Bleeding of the ink in crevasses in the substrate is seen in figure 1(b) for example. Further examples of printing on the elastomeric substrate used is shown in figure S3. There is bleeding due to surface morphology and possibly due to surface energy differential between the rubber and water. Once the ink dries the graphene forms a random network embedded in the natural rubber matrix. An SEM of as deposited ink is available in fig S4 showing random distribution of Graphene in the natural rubber.

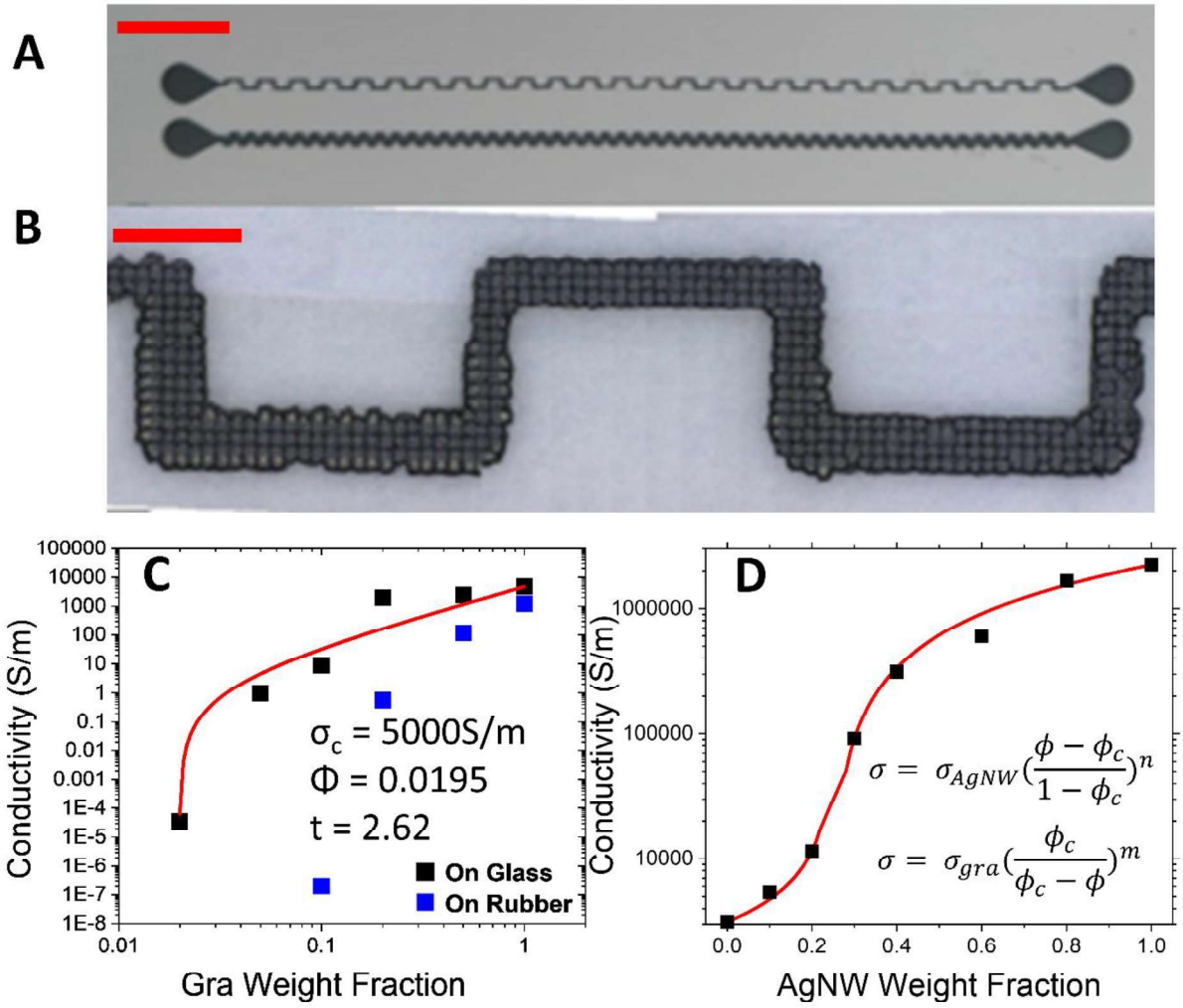

Figure 1 a) Single pass screen print on paper substrate (scale bar = 2cm). (b) Micrograph of thinner track form (e) (e) (scale bar = 200um) (c) Conductivity of Natural Rubber/Graphene composite with increasing graphene weight fraction. (d) Conductivity of silver nanowires forming percolating network in graphene

To allow accurate readout of currents at low potentials to retrieve strain, the conductivity of the printed material must be sufficiently high given the geometry of the device due to it being printed. To understand the behaviour of conductivity of natural rubber/graphene (NR/Gra) composites films of different mass fractions of graphene are prepared and screen-printed onto a glass substrate. Percolation theory describes the formation of conductive pathways through an insulating medium. Once the material exceeds the percolation threshold the conductivity increases exponentially until it reaches the conductivity of the filler material following the equation 3.

$$\sigma = \sigma_f \left(\frac{\phi - \phi_0}{1 - \phi_0} \right) \qquad \text{Equation 3}$$

Where σ and ϕ represent conductivities and volume fractions respectively, ϕ_c is the conductivity of the filler material, ϕ_c is the percolation threshold at which a conductive pathway across the material is formed, and n is a percolation exponent which can be related to the dimensionality of the system. Figure 1c shows the percolation curve of graphene in natural rubber on glass substrate which has a percolation threshold of 0.0195 and an exponent of 2.62 which is appropriate for randomly oriented materials in a 2D matrix. The filler conductivity is around 5000 S/m. A 50 wt.% graphene composite was chosen for subsequent electromechanical applications as the conductivity (~3000 S/m), is with a factor of 2 of the graphene only sample resulting in minimal resistive losses. This is high for liquid exfoliated graphite composites but at the low end of many conductive composites[14,15,25,26]. These composites achieve high conductivities by using carbon nanotubes[25], graphene[27], metal nanomaterials[15,28] or conductive polymers[29] (See table 1 in SI for values). However, few of these systems are printable thus requiring further formulation to become suitable. Furthermore, once printed due to the roughness of the printed exhibited in figure 1(b) and the roughness of the substrate deviations in conductivity occur resulting in higher percolation thresholds, estimated to be around 10%, and lower conductivities due to finite size scaling[30].

Due to the high conductivity and aspect ratio of AgNWs, AgNWs may produce lower resistance printed tracks allowing for lower potentials for strain sensing. To understand the effect of addition of AgNW and graphene to natural rubber the mixing of silver nanowires into graphene first had to be understood. Adding silver nanowires to graphene produces as percolation curve similar to that of a conductor in another conductor due to the relative conductivities of the materials differing by only 3 orders of magnitude[31]. Figure 1d shows the increase in conductivity due to the addition of the nanowires with a higher percolation

threshold of 25 wt.%. Below that threshold conductivity follows different behaviour described by the following equation.

$$\sigma = \sigma_m \left(\frac{\phi_0}{\phi_0 - \phi} \right)^p \qquad \text{Equation 4}$$

Where σ_m is the conductivity of the matrix, in this case Graphene, and p is the percolation exponent. Due to the high cost of AgNWs a mass fraction of 15 wt.% was decided upon in order to balance performance and cost. Additionally, high fractions of AgNW composites could weld at nanowire-nanowire junctions that are susceptible to brittle fracture under strain. This ink produces a film with a conductivity of 30,000 S/m. The addition of the AgNWs dramatically reduced the resistance of the printed films as expected. Interestingly, however, the dependence of resistance on thickness as shown in figure 1f is now mostly scatter having minimised the interruption of conductive pathways using the silver nanowires.

Percolative networks in elastomers have been reported as strain gauges[1]. Effective strain gauges are required in many current technologies and more robust, stretchable and sensitive strain gauges could enable new technologies. At low strains most materials exhibit linear resistance relationships with strain. A variety of NR/Gra composites also exhibits this low strain linearity as shown in figure 2a. The response of the NR/Gra/AgNW is shown in the inset. The resistance increases linearly until a critical point at which deviation resultant of deformation of the material occurs (shown in figure S5). This phenomenon has been linked with the yield strain of the material and is called the working factor[2]. Both gauge factor and working factor of the respective composites are shown if figure 2(b). The printed tracks with 50% weight graphene show significantly higher gauge factors of 117 and the best working factor. The sharp decay in gauge factor can be attributed to the effect of the lower

conductivity as particle separation in low weight fraction composites allows for more dramatic conductivity changes. The NR/Gra/AgNW printed tracks displayed a lower gauge factor of 17 (shown in figure S5). The gauge factor of the first strain in these systems is typically on the order of 2-3 for metal foil resistors while graphene infused elastic bands exhibit gauge factors of 40[1] and further research has yielded successively higher gauge factors[2,3].

Generally, the practical operation parameters of strain gauges are not limited to a single strain or even strains below 2%. A main consideration of the material must be the ability to sustain a wide range of strains as well as multiple repetitions. Measuring the resistance of films before and after straining from low strains to up to 50% shows how the resistance of the 50 wt% NR/Gra films recover up to 20% (figure 2c). However, the higher weight fraction of graphene results in irreversible damage at much lower strains and screen-printed graphene tracks noticeably peeled of the substrate even at very low strains. For the 50wt% sample once the limit of 20% strain was exceeded there was an increase in resistance after the material is returned to the unstrained state. The breakdown in resistance is due to irreversible breaking or deformation of the film as high mass fraction composites generally have reduced strain at break compared to composites of lower filler mass fractions[8]. To this end all further work was performed on either 50:50 NR/Gra or 50:33.33:16.67 NR/Gra/AgNW tracks printed on the elastomer composite.

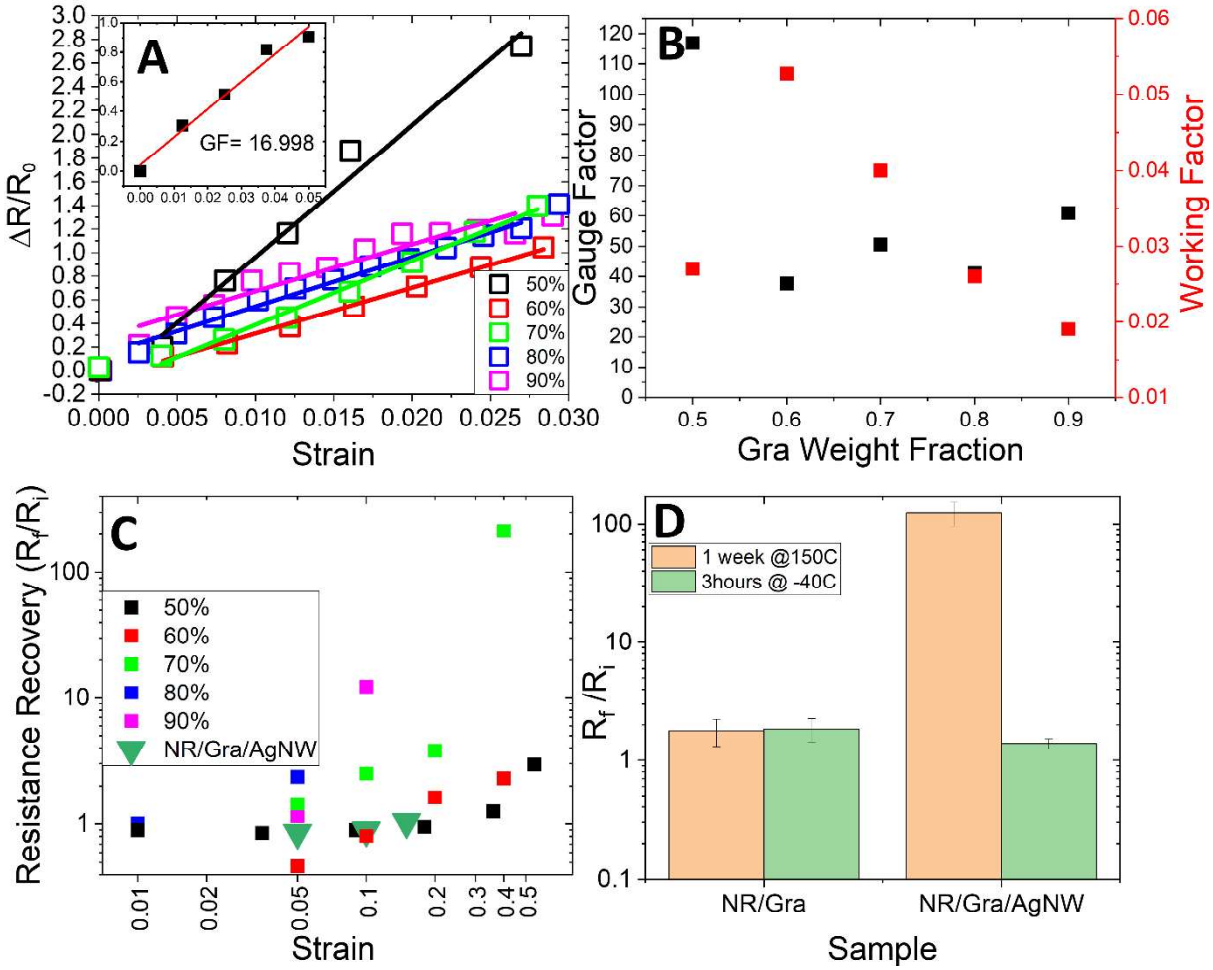

Figure 2 (a) ΔR/R0 variation with strain for composites of differing graphene loading.(Inset) ΔR/R0 of NR/Gra/AgNW Composite(b) Variation of gauge and working factors with graphene weight fraction(c) Recovery of resistance after 10 cycles to a maximum strain (d) Recovery of resistance after temperature treatment of unstrained samples. NR/Gra = (50:50) and NR/Gra/AgNW = (50:33.33:16.67)

For many industrial applications elastomeric belts are close to engines which operate at elevated temperatures. Automotives may be outdoors in extremely low temperatures. Taking this into account any printable conductive track must be robust to storage and operation in a wide range of temperatures. The conductivity of graphene is robust to temperatures much higher than the breakdown of traditional elastomers, which is typically up to 200 °C, making these composites well suited to elevated temperatures in automotive vehicles. For such temperatures, the thermal expansivity mismatch between substrate and film is the main issue and can cause delamination. Figure 2d illustrates the impact of heating and chilling on NR/Gra films which generally stay within a factor of 2 after storage at 150 ºC. AgNWs,

however, are not as robust under elevated temperature usually forming silver oxide particles when exposed to unfavourable conditions. This is observed in the NR/Gra/AgNWs composites under high temperatures with breakdown of electrical conductivity resulting in resistance increases by a factor of ~70 effectively the same conductivity of the NR/Gra composites.

For low temperatures, only mismatch of thermal expansivity is considered as most processes which degrade conductivity are thermally activated. As such, most of the printed tracks on both the graphene and graphene/AgNW in natural rubber remain within a factor of 2 of the original resistance values after storage at -40 ºC for 3 hours (figure 2d).

Many elastomeric materials are used in dynamic processes, belts in engines for example. This requires material that preserves performance over extended cycling. The combination of conductivity and the sustenance of high strains without degradation of performance suggests that the printed tracks are suitably placed to occupy this niche. Simultaneous mechanical straining with current monitoring allows tracking of the materials performance in the dynamic state. Figure 3a shows the typical behaviour of the resistance of films when the substrate is strained. When a material is strained the resistance increases due to separation of conductive fillers as stated previously. Similarly, the current levels return to a maximum when the material is unstrained. Under dynamic conditions, however, this maximum current does not correspond to the resistance of the unstrained state. This is due to the filler particles having mobility in the matrix requiring further relaxation. The resistance also undergoes a decay process, which we attribute to the mobility of the filler. Once cycling stops the material returns to a resistance close to the starting resistance, occasionally this resistance is lower. This suggests dynamic agitation allows for optimising of the orientation of the filler particles.

The robust character of the material allows the resistance to return to values close to the initial resistance after many cycles even at high temperatures shown in figure S6(a&b).

By observing the oscillations of the resistance in figure 3(a) at a point where the decay of resistance has ceased one can take the maximum and minimum resistance (Rmax and Rmin) and substitute them into equation 1. Where ΔR is Rmax - Rmin and R0 is Rmin. This yields a "dynamic gauge factor" (DGF) which allows for assessment of maximum strain value while a device is cycling. By analysing this DGF with strain as shown in Figure 3(b) it can be shown to be uniform over this strain range allowing for in situ diagnostics. The DGF for the NR/Gra composite is around 7 and the NR/Gra/AgNWs is higher at approximately 9. These DGF are significantly lower than the single strain measurements. This is due to the combination of two effects. The first being the rate dependence of the gauge factor. This is a poorly studied phenomenon. A rate change of an order of magnitude between the single strain and the cyclic strain measurements, as applied in this study, results in a different gauge factor. In addition to this figure 3(a) shows a dramatically higher change in resistance in the first strain compared to subsequent cycles from which the DGF is defined.

After extensive cycling there are no macroscopic changes to the material and conductivity in some cases has even improved. On further examination, in figure 3(c), using scanning electron microscopy the onset of delamination is observed on a sample strained to 15% 1,000,000 times with a comparison to the unstrained sample shown on the inset. However seeing as the resistance changes for 1,000, 100,000, and 1,000,000 cycles are similar, shown in figure S7(c), the major morphological changes happen within the initial strains and the material remains robust thereafter.

Figure 3(d) provides benchmarking against a variety of stretchable materials that retain conductivity after straining. These conductors are fabricated using a variety of materials and generally are polymer composites

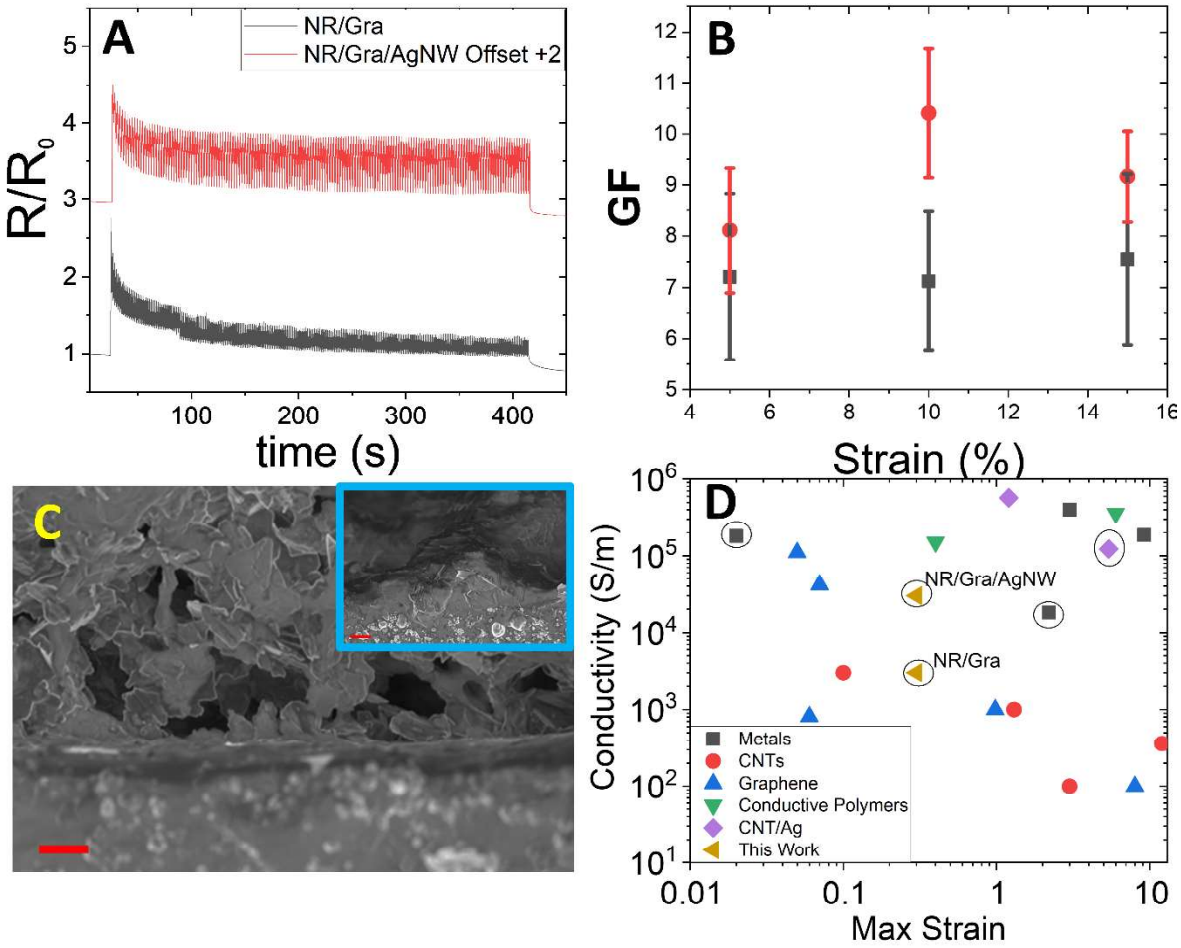

Figure 3 (a) Real time straining to 5% of NR/Gra and NR/Gra/AgNW for 1000 cycles (b) Peak to peak effective gauge factors for all films for a range of strains at room temperature (c) SEM of edge of composite after 100000 strain cycles at 15% (inset) SEM of edge with no straining (scale bars = 1μm) (d) Comparison of conductivity and stretchability of various liquid processable conductors. Circles indicate a demonstration of printing.[1,6,14,24–28,30–37]

or on a polymer substrate. The materials include CNTs, graphene and metal nanostructures. and conductive polymers. Materials that have had printing demonstrated are indicated with black circles. While excellent conductivity and stretchability is possible, all of these are conductive polymers and or a significant metal component. Full list of properties shown in table 1 in SI. In comparison, the NR/Gra printed track shows modest conductivity and

stretchability but has been demonstrated benefits from simplicity in fabrication as well as being comprised of relatively cheap materials. Addition of AgNWs improves the conductivity significantly for high tech applications where exposure to high temperatures is not a concern.

4. Conclusions

Using natural rubber to help bind and promote adhesion of conductive nanomaterials to elastomeric substrates allows for printed tracks that are conductive, stretchable with conductivity being sensitive to the strain. The materials are tested under a wide range of environmental and operational conditions and exhibited comparable performance at temperatures as high as 150º C. The combination of reasonable conductivity along with robust performance at high strains and temperatures allow for a range of applications and are particularly suited for printing onto automotive components. For high conductivity applications silver nanowires can also be added to these systems and similar performance under strain is reported. Silver nanowires, while effective, have limited performance at elevated temperatures due to oxidation limiting operation to devices that are not expected to diverge from room temperature. Otherwise the material studied shows promise as a printable solution for integrating electrical components onto a variety of elastomeric substrates as either strain sensors or components that need to survive straining.

Acknowledgements

Funding for this work was provided through AMD. ABD thanks University of Sussex for funding through the strategic development fund.

References

[1] C.S. Boland, U. Khan, C. Backes, A. O'Neill, J. McCauley, S. Duane, R. Shanker, Y. Liu, I. Jurewicz, A.B. Dalton, J.N. Coleman, Sensitive, High-Strain, High-Rate Bodily Motion Sensors Based on Graphene–Rubber Composites, ACS Nano. 8 (2014) 8819–8830. https://doi.org/10.1021/nn503454h.

[2] C.S. Boland, Stumbling through the Research Wilderness, Standard Methods To Shine Light on Electrically Conductive Nanocomposites for Future Healthcare Monitoring, ACS Nano. 13 (2019) 13627–13636. https://doi.org/10.1021/acsnano.9b06847.

[3] M. Amjadi, K.-U. Kyung, I. Park, M. Sitti, Stretchable, Skin-Mountable, and Wearable Strain Sensors and Their Potential Applications: A Review, Adv. Funct. Mater. 26 (2016) 1678–1698. https://doi.org/10.1002/adfm.201504755.

[4] S. Iijima, Helical microtubules of graphitic carbon, Nature. 354 (1991) 56–58. https://doi.org/10.1038/354056a0.

[5] J.N. Coleman, U. Khan, Y.K. Gun'ko, Mechanical Reinforcement of Polymers Using Carbon Nanotubes, Advanced Materials. 18 (2006) 689–706. https://doi.org/10.1002/adma.200501851.

[6] S. Zhao, J. Li, D. Cao, Y. Gao, W. Huang, G. Zhang, R. Sun, C.-P. Wong, Percolation threshold-inspired design of hierarchical multiscale hybrid architectures based on carbon nanotubes and silver nanoparticles for stretchable and printable electronics, J. Mater. Chem. C. 4 (2016) 6666–6674. https://doi.org/10.1039/C6TC01728B.

[7] A.K. Geim, K.S. Novoselov, THE RISE OF GRAPHENE, (n.d.) 14.

[8] D.G. Papageorgiou, I.A. Kinloch, R.J. Young, Mechanical properties of graphene and graphene-based nanocomposites, Progress in Materials Science. 90 (2017) 75–127. https://doi.org/10.1016/j.pmatsci.2017.07.004.

[9] X.-Y. Qi, D. Yan, Z. Jiang, Y.-K. Cao, Z.-Z. Yu, F. Yavari, N. Koratkar, Enhanced Electrical Conductivity in Polystyrene Nanocomposites at Ultra-Low Graphene Content, ACS Applied Materials & Interfaces. 3 (2011) 3130–3133. https://doi.org/10.1021/am200628c.

[10] W. Bauhofer, J.Z. Kovacs, A review and analysis of electrical percolation in carbon nanotube polymer composites, Composites Science and Technology. 69 (2009) 1486–1498. https://doi.org/10.1016/j.compscitech.2008.06.018.

[11] Y. Sun, Y. Yin, B.T. Mayers, T. Herricks, Y. Xia, Uniform Silver Nanowires Synthesis by Reducing $AgNO_3$ with Ethylene Glycol in the Presence of Seeds and Poly(Vinyl Pyrrolidone), Chemistry of Materials. 14 (2002) 4736–4745. https://doi.org/10.1021/cm020587b.

[12] L. Hu, H.S. Kim, J.-Y. Lee, P. Peumans, Y. Cui, Scalable Coating and Properties of Transparent, Flexible, Silver Nanowire Electrodes, ACS Nano. 4 (2010) 2955–2963. https://doi.org/10.1021/nn1005232.

[13] M. Cann, M.J. Large, S.J. Henley, D. Milne, T. Sato, H. Chan, I. Jurewicz, A.B. Dalton, High performance transparent multi-touch sensors based on silver nanowires, Materials Today Communications. 7 (2016) 42–50. https://doi.org/10.1016/j.mtcomm.2016.03.005.

[14] K.-Y. Chun, Y. Oh, J. Rho, J.-H. Ahn, Y.-J. Kim, H.R. Choi, S. Baik, Highly conductive, printable and stretchable composite films of carbon nanotubes and silver, Nature Nanotechnology. 5 (2010) 853–857. https://doi.org/10.1038/nnano.2010.232.

[15] Y. Cheng, R. Wang, J. Sun, L. Gao, Highly Conductive and Ultrastretchable Electric Circuits from Covered Yarns and Silver Nanowires, ACS Nano. 9 (2015) 3887–3895. https://doi.org/10.1021/nn5070937.

[16] C. Gabbett, C.S. Boland, A. Harvey, V. Vega-Mayoral, R.J. Young, J.N. Coleman, The Effect of Network Formation on the Mechanical Properties of 1D:2D Nano:Nano Composites, Chem. Mater. 30 (2018) 5245–5255. https://doi.org/10.1021/acs.chemmater.8b01945.

[17] M. Hirata, T. Gotou, S. Horiuchi, M. Fujiwara, M. Ohba, Thin-film particles of graphite oxide 1:: High-yield synthesis and flexibility of the particles, Carbon. 42 (2004) 2929–2937. https://doi.org/10.1016/j.carbon.2004.07.003.
[18] Y. Hernandez, V. Nicolosi, M. Lotya, F.M. Blighe, Z. Sun, S. De, I.T. McGovern, B. Holland, M. Byrne, Y.K. Gun'Ko, J.J. Boland, P. Niraj, G. Duesberg, S. Krishnamurthy, R. Goodhue, J. Hutchison, V. Scardaci, A.C. Ferrari, J.N. Coleman, High-yield production of graphene by liquid-phase exfoliation of graphite, Nature Nanotech. 3 (2008) 563–568. https://doi.org/10.1038/nnano.2008.215.
[19] M. Lotya, Y. Hernandez, P.J. King, R.J. Smith, V. Nicolosi, L.S. Karlsson, F.M. Blighe, S. De, Z. Wang, I.T. McGovern, G.S. Duesberg, J.N. Coleman, Liquid Phase Production of Graphene by Exfoliation of Graphite in Surfactant/Water Solutions, J. Am. Chem. Soc. 131 (2009) 3611–3620. https://doi.org/10.1021/ja807449u.
[20] E. Jabari, F. Ahmed, F. Liravi, E.B. Secor, L. Lin, E. Toyserkani, 2D printing of graphene: a review, 2D Materials. 6 (2019) 042004. https://doi.org/10.1088/2053-1583/ab29b2.
[21] Q. Huang, Y. Zhu, Printing Conductive Nanomaterials for Flexible and Stretchable Electronics: A Review of Materials, Processes, and Applications, Advanced Materials Technologies. 4 (2019) 1800546. https://doi.org/10.1002/admt.201800546.
[22] M.J. Large, S.P. Ogilvie, A.A. Graf, P.J. Lynch, M.A. O'Mara, T. Waters, I. Jurewicz, J.P. Salvage, A.B. Dalton, Large-Scale Surfactant Exfoliation of Graphene and Conductivity-Optimized Graphite Enabling Wireless Connectivity, Advanced Materials Technologies. n/a (n.d.) 2000284. https://doi.org/10.1002/admt.202000284.
[23] C. Backes, K.R. Paton, D. Hanlon, S. Yuan, M.I. Katsnelson, J. Houston, R.J. Smith, D. McCloskey, J.F. Donegan, J.N. Coleman, Spectroscopic metrics allow in situ measurement of mean size and thickness of liquid-exfoliated few-layer graphene nanosheets, Nanoscale. 8 (2016) 4311–4323. https://doi.org/10.1039/C5NR08047A.
[24] U. Khan, A. O'Neill, M. Lotya, S. De, J.N. Coleman, High-Concentration Solvent Exfoliation of Graphene, Small. 6 (2010) 864–871. https://doi.org/10.1002/smll.200902066.
[25] S. Ata, K. Kobashi, M. Yumura, K. Hata, Mechanically Durable and Highly Conductive Elastomeric Composites from Long Single-Walled Carbon Nanotubes Mimicking the Chain Structure of Polymers, Nano Letters. 12 (2012) 2710–2716. https://doi.org/10.1021/nl204221y.
[26] S. Choi, S.I. Han, D. Kim, T. Hyeon, D.-H. Kim, High-performance stretchable conductive nanocomposites: materials, processes, and device applications, Chem. Soc. Rev. 48 (2019) 1566–1595. https://doi.org/10.1039/C8CS00706C.
[27] Z. Chen, W. Ren, L. Gao, B. Liu, S. Pei, H.-M. Cheng, Three-dimensional flexible and conductive interconnected graphene networks grown by chemical vapour deposition, Nature Materials. 10 (2011) 424–428. https://doi.org/10.1038/nmat3001.
[28] K.-S. Kim, K.-H. Jung, S.-B. Jung, Design and fabrication of screen-printed silver circuits for stretchable electronics, Microelectronic Engineering. 120 (2014) 216–220. https://doi.org/10.1016/j.mee.2013.07.003.
[29] Y. Wang, C. Zhu, R. Pfattner, H. Yan, L. Jin, S. Chen, F. Molina-Lopez, F. Lissel, J. Liu, N.I. Rabiah, Z. Chen, J.W. Chung, C. Linder, M.F. Toney, B. Murmann, Z. Bao, A highly stretchable, transparent, and conductive polymer, Science Advances. 3 (2017) e1602076. https://doi.org/10.1126/sciadv.1602076.
[30] S.F. Wang, A.A. Ogale, Continuum space simulation and experimental characterization of electrical percolation behavior of particulate composites, Composites Science and Technology. 46 (1993) 93–103. https://doi.org/10.1016/0266-3538(93)90165-D.
[31] G. Cunningham, M. Lotya, N. McEvoy, G.S. Duesberg, P. van der Schoot, J.N. Coleman, Percolation scaling in composites of exfoliated MoS2 filled with nanotubes and graphene, Nanoscale. 4 (2012) 6260–6264. https://doi.org/10.1039/C2NR31782F.